

On a probabilistic approach to synthesize control policies from example datasets

Davide Gagliardi ^a, Giovanni Russo ^b

^a*School of Electrical and Electronic Engineering, University College Dublin, Ireland (e-mail: davide.gagliardi@ucd.ie).*

^b*Department of Information and Electrical Engineering and Applied Mathematics, University of Salerno, Italy (e-mail: giovarusso@unisa.it).*

Abstract

This paper is concerned with the design of control policies from example data. The case considered is when only a probabilistic characterization of the system to be controlled is available and the system is affected by actuation constraints. These constraints are unknown to the demonstrators and hence might not be satisfied in the possibly noisy example data. In this context, we introduce a number of theoretical results to compute a control policy from the examples that: (i) makes the behavior of the closed-loop system similar to the one illustrated in the dataset; (ii) guarantees compliance with the constraints. The theoretical results give an explicit expression for the control policy and this allows to turn our findings into an algorithmic procedure. The procedure gives a systematic tool to compute the policy. The effectiveness of our approach is illustrated via a numerical example, where we use real data collected from test drives to synthesize a control policy for the merging of a car on a highway.

1 Introduction

Model-based control is a key paradigm to design control systems: the design of platoons (Stdli et al., 2017), fault tolerant (LeBlanc et al., 2013) and biochemical systems (DelVecchio et al., 2018) are just few of the frontier applications where this approach has been successfully used. Unfortunately, detailed mathematical models in the form of e.g. differential/difference equations, are not always available and, when available, can be hard to identify. Hence, a paradigm that is becoming increasingly popular is to synthesize control policies directly from data, see e.g. (Van Waarde et al., 2020; Hou and Wang, 2013) and references therein. This approach, which aims at designing policies while bypassing the need to devise/identify a mathematical model, can be useful in applications where first-principle models cannot be obtained and where system identification is too computationally expensive (Van Waarde et al., 2020).

An appealing framework to design controllers from data is that of using demonstrations. This *learning from demonstrations* approach involves learning a sequence of actions by observing an expert (Hanawal et al., 2019; Wabersich and Zeilinger, 2018; Zhu et al., 2020). In this context, a key challenge is the design of policies from noisy datasets for systems affected by actuation constraints. These constraints might be unknown to (and hence not fulfilled by) the demonstrators. Motivated by

this, we present ¹ a set of technical results to synthesize policies from noisy examples for systems for which only a probabilistic characterization is known. The policies found with our results make the controlled system similar to the behavior illustrated in the examples while, at the same time, guarantee the fulfillment of the constraints. We now briefly survey some related works on data-driven control and learning from demonstrations.

Data-driven control. As noted in e.g. (Van Waarde et al., 2020), work on data-driven control can be traced back to (Ziegler and Nichols, 1942) and their results on the tuning of PID controllers. Recently, driven by the explosion in the *amount* of available data, the problem of finding control policies from datasets has gained increasing attention, see e.g. (Hou and Xu, 2009). For example, in (Tanaskovic et al., 2017) a direct data-driven design approach is introduced for discrete-time stabilizable systems with Lipschitz nonlinearities, while works such as (Markovsky and Rapisarda, 2007; Goncalves da Silva et al., 2019; Baggio et al., 2019) consider the problem of designing optimal controllers for systems that have an underlying linear dynamics. Besides works on e.g. self-tuning controllers (Keel and Bhattacharyya, 2008) other remarkable results have been obtained by taking

¹ An early version of a special case of the results introduced here presented, without proofs, as an extended abstract at the 21st IFAC World Congress (Gagliardi and Russo, 2020).

inspiration from the rich literature on Model Predictive Control (MPC). These include (Rosolia and Borrelli, 2018), where an MPC learning algorithm is introduced for iterative tasks when the system dynamics is partially known, (Salvador et al., 2018) where a data-based predictive control algorithm is presented for unknown time-invariant systems and (Coulson et al., 2019; Coulson et al., 2019) that, by taking a behavioral systems perspective, introduce a data-enabled predictive control algorithm for data generated by LTI systems.

Learning from demonstrations. At their roots, learning from demonstration techniques largely rely on inverse optimal control (Bryson, 1996). Nowadays, these techniques are recognized as a convenient framework to learn parametrized policies from *success stories* (Argall et al., 2009) and potential applications include planning (Englert et al., 2017) and medical prescriptions learning (Xu and Paschalidis, 2019; Hanawal et al., 2019). There is then no surprise that, over the years, a number of techniques have been developed to tackle the problem of learning parametrized control policies from demonstrations, mainly in the context of Markov Decision Processes (Sutton and Barto, 1998). Results include (Ratliff et al., 2009), which leverages a linear programming approach, (Ratliff et al., 2006) which relies on a maximum margin approach, (Ziebart et al., 2008) that makes use of the maximum entropy principle and (Ramachandran and Amir, 2007) that formalizes the problem via Bayesian statistics. Finally, a Bayesian approach (Peterka, 1981) to dynamical systems is also at the basis of works such as (Kárný, 1996; Kárný and Guy, 2006; Herzallah, 2015; Pegueroles and Russo, 2019; Krn and Kroupa, 2012), which formalize the control problem as the problem of minimizing a cost function that captures the discrepancy between an ideal probability density function and the actual probability density function of the system under control.

Contributions of this paper

We introduce a framework to design policies from example data for systems having actuation constraints unknown to the demonstrators and for which only a probabilistic description is known. Our contributions are summarized as follows:

- inspired by a probabilistic approach to dynamical systems, we formalize the problem of computing control policies from noisy example data as the problem of *reshaping* certain probability density functions obtained directly from the available dataset. We explicitly embed actuation constraints in our probabilistic formulation and this leads to a constrained control problem;
- to tackle this problem, we introduce a number of theoretical results to compute the policy so that the controlled system has a behavior similar to the one illustrated in the examples and, at the same time, satisfies

its constraints. The results, which give an explicit expression for the control policy, leverage a probabilistic description of the system and hence its underlying dynamics can be unknown, nonlinear and stochastic;

- the results are turned into an algorithmic procedure and this gives a systematic tool to effectively compute the control policy;
- finally, we illustrate the effectiveness of the results via a numerical example that involves the use of real data.

2 Mathematical Preliminaries

2.1 Notation

Sets, as well as operators, are denoted by *calligraphic* characters, while vector quantities are denoted in **bold**. Let d_z be a positive integer and consider the measurable space $(\mathcal{Z}, \mathcal{F}_z)$, with $\mathcal{Z} \subseteq \mathbb{R}^{d_z}$ and with \mathcal{F}_z being a σ -algebra on \mathcal{Z} . Then, the random (row) vector (i.e. a multidimensional random variable) on $(\mathcal{Z}, \mathcal{F}_z)$ is denoted by \mathbf{Z} and its realization is denoted by \mathbf{z} . The *probability density function* (or simply *pdf* in what follows) of a continuous \mathbf{Z} is denoted by $f_{\mathbf{Z}}(\mathbf{z})$. For notational convenience, whenever it is clear from the context, we omit the argument and/or the subscript of the pdf. Hence, the support of $f := f_{\mathbf{Z}}(\mathbf{z})$ is denoted by $S(f)$ and, analogously, the expectation of a function $\mathbf{h}(\cdot)$ of \mathbf{Z} is indicated with $\mathbb{E}_f[\mathbf{h}(\mathbf{Z})]$ and defined as $\mathbb{E}_f[\mathbf{h}(\mathbf{Z})] := \int_{S(f)} \mathbf{h}(\mathbf{z})f(\mathbf{z})d\mathbf{z}$. We also remark here that: (i) whenever we apply the averaging operator to a given function, we use an upper-case letter for the function argument as this is a random vector; (ii) to stress the linearity of certain functionals or operators with respect to a specific argument, we include that argument in square brackets. The *joint* pdf of two random vectors, say \mathbf{Z} and \mathbf{Y} , is denoted by $f_{[\mathbf{Z}, \mathbf{Y}]}(\mathbf{z}, \mathbf{y})$ and abbreviated with $f(\mathbf{z}, \mathbf{y})$. The *conditional* probability density function (or *cpdf* in what follows) of \mathbf{Z} with respect to the random vector \mathbf{Y} is denoted by $f(\mathbf{z}|\mathbf{y})$ and, whenever the context is clear, we use the shorthand notation $\tilde{f}_{\mathbf{Z}}$. Finally, given $\mathcal{Z} \subseteq \mathbb{R}^{d_z}$, its *indicator function* is denoted by $\mathbb{1}_{\mathcal{Z}}(\mathbf{z})$. That is, $\mathbb{1}_{\mathcal{Z}}(\mathbf{z}) = 1, \forall \mathbf{z} \in \mathcal{Z}$ and 0 otherwise. We also make use of the internal product between tensors, which is denoted by $\langle \cdot, \cdot \rangle$, while $\mathcal{A} \setminus \mathcal{B}$ is the set difference between \mathcal{A} and \mathcal{B} . We indicate countable sets as $\{w_k\}_{k=k_1}^{k_n}$, where w_k is the generic element belonging to the set and k_1, k_n are the indices of the first and last element respectively. We denote by $\mathcal{K} := \{k\}_{k=k_1}^{k_n}$ (or simply $\{k\}_{k_1}^{k_n}$) the set of consecutive integers between k_1 and k_n . Hence, the set $\{w_k\}_{k=k_1}^{k_n} := \{w_k\}_{k \in \mathcal{K}}$ can be compactly written as $\{w_k\}_{\mathcal{K}}$.

2.2 The Kullback-Leibler divergence

The control problem considered in this paper will be stated (see Section 3.1) in terms of the Kullback-Leibler

(KL, (Kullback and Leibler, 1951)) divergence, formalized with the following:

Definition 1 (Kullback-Leibler(KL) divergence)

Consider two pdfs, $\phi := \phi_{\mathbf{Z}}(\mathbf{z})$ and $g := g_{\mathbf{Z}}(\mathbf{z})$, with ϕ being absolutely continuous with respect to g . Then, the KL-divergence of ϕ with respect to g is

$$\mathcal{D}_{KL}(\phi||g) := \int_{S(\phi)} \phi \ln \left(\frac{\phi}{g} \right) d\mathbf{z}. \quad (1)$$

Intuitively, $\mathcal{D}_{KL}(\phi||g)$ is a measure of how well ϕ approximates g . We now give a property of the KL-divergence, the KL-divergence splitting property, which is used in the proof of Theorem 1.

Property 1 Let ϕ and g be two pdfs of the random vector $[\mathbf{Z}, \mathbf{Y}]$, with \mathbf{Z} and \mathbf{Y} being random vectors of dimensions n^Z and n^Y , respectively. Then, the following splitting rule holds:

$$\begin{aligned} \mathcal{D}_{KL}(\phi(\mathbf{y}, \mathbf{z})||g(\mathbf{y}, \mathbf{z})) &= \\ &= \mathcal{D}_{KL}(\phi(\mathbf{y})||g(\mathbf{y})) + \mathbb{E}_{\phi(\mathbf{Y})} [\mathcal{D}_{KL}(\phi(\mathbf{z}|\mathbf{Y})||g(\mathbf{z}|\mathbf{Y}))] \end{aligned} \quad (2)$$

Proof: The proof follows from the definition of \mathcal{D}_{KL} , the conditioning and independence rules for pdfs. The complete proof is given in the appendix. \square

3 Formulation of the Control Problem

Let: (i) $\mathcal{K} := \{k\}_{k=1}^n$, $\mathcal{K}_0 := \mathcal{K} \cup \{0\}$ and $\mathcal{T} := \{t_k : k \in \mathcal{K}_0\}$ be the time horizon over which the system is observed; (ii) $\mathbf{x}_k \in \mathbb{R}^{d_x}$ and $\mathbf{u}_k \in \mathbb{R}^{d_u}$ be, respectively, the system state and input at time $t_k \in \mathcal{T}$; (iii) $\mathbf{d}_k := (\mathbf{x}_k, \mathbf{u}_k)$ be the data collected from the system at time $t_k \in \mathcal{T}$ and \mathbf{d}^k the data collected from $t_0 \in \mathcal{T}$ up to time $t_k \in \mathcal{T}$ ($t_k > t_0$). As shown in e.g. (Peterka, 1981), the system behavior can be described via the joint pdf of the observed data, say $f(\mathbf{d}^n)$. Moreover, the chain rule for pdfs leads to the following factorization for $f(\mathbf{d}^n)$:

$$f(\mathbf{d}^n) = \prod_{k \in \mathcal{K}} f(\mathbf{x}_k|\mathbf{u}_k, \mathbf{x}_{k-1}) f(\mathbf{u}_k|\mathbf{x}_{k-1}) f(\mathbf{x}_0). \quad (3)$$

Throughout this work we refer to (3) as the *probabilistic description of the closed loop system*, or we simply say that (3) is our *closed loop system*.

Remark 1 The cpdf $f(\mathbf{x}_k|\mathbf{u}_k, \mathbf{x}_{k-1})$ describes the system behavior at time t_k , given the previous state and the input at time t_k . The input is generated by the cpdf $f(\mathbf{u}_k|\mathbf{x}_{k-1})$. This is a randomized control policy returning the input given the previous state. Note that the initial conditions are embedded in the probabilistic system description through the prior $f(\mathbf{x}_0)$.

In the rest of the paper we use the following *shorthand* notations: $\tilde{f}_{\mathbf{X}}^k := f(\mathbf{x}_k|\mathbf{u}_k, \mathbf{x}_{k-1})$, $\tilde{f}_{\mathbf{U}}^k := f(\mathbf{u}_k|\mathbf{x}_{k-1})$, $\tilde{f}^k := \tilde{f}_{\mathbf{X}}^k \tilde{f}_{\mathbf{U}}^k$, $f_0 := f(\mathbf{x}_0)$ and $f^n := f(\mathbf{d}^n)$. Hence, (3) can be compactly written as

$$f^n = \prod_{k \in \mathcal{K}} \tilde{f}_{\mathbf{X}}^k \tilde{f}_{\mathbf{U}}^k f_0 = \tilde{f}_1^n f_0, \quad \tilde{f}_1^n := \prod_{k \in \mathcal{K}} \tilde{f}_{\mathbf{X}}^k \tilde{f}_{\mathbf{U}}^k. \quad (4)$$

3.1 The control problem

Our goal is to synthesize, from an example dataset, say \mathbf{d}_e^n , the control pdf/policy, $f(\mathbf{u}_k|\mathbf{x}_{k-1})$, that: (i) makes the closed loop system *similar* to the behavior illustrated in the data; (ii) satisfies the system actuation constraints even if these are not fulfilled by the examples. We specify the behavior illustrated in the examples through the reference pdf $g(\mathbf{d}_e^n)$ extracted from the example dataset. Note that $g(\mathbf{d}_e^n)$ can always be computed as e.g. the empirical distribution of the available data. Following the chain rule for pdfs we have $g(\mathbf{d}_e^n) := \prod_{k \in \mathcal{K}} g(\mathbf{x}_k|\mathbf{u}_k, \mathbf{x}_{k-1}) g(\mathbf{u}_k|\mathbf{x}_{k-1}) g(\mathbf{x}_0)$. Again, by setting $\tilde{g}_{\mathbf{X}}^k := g(\mathbf{x}_k|\mathbf{u}_k, \mathbf{x}_{k-1})$, $\tilde{g}_{\mathbf{U}}^k := g(\mathbf{u}_k|\mathbf{x}_{k-1})$, $\tilde{g}^k := \tilde{g}_{\mathbf{X}}^k \tilde{g}_{\mathbf{U}}^k$, $g_0 := g(\mathbf{x}_0)$ and $g^n := g(\mathbf{d}_e^n)$ we get:

$$g^n = \prod_{k \in \mathcal{K}} \tilde{g}_{\mathbf{X}}^k \tilde{g}_{\mathbf{U}}^k g_0 = \tilde{g}_1^n g_0, \quad \tilde{g}_1^n := \prod_{k \in \mathcal{K}} \tilde{g}_{\mathbf{X}}^k \tilde{g}_{\mathbf{U}}^k. \quad (5)$$

The control problem, formalized next, can then be recast as the problem of designing $f(\mathbf{u}_k|\mathbf{x}_{k-1})$ so that f^n approximates g^n . This is formally stated as follows:

Problem 1 Let, $\forall k \in \mathcal{K}$:

- (i) n_e^k and n_l^k be positive integers;
- (ii) $\mathbf{u} \mapsto h_{\mathbf{u},j}^k(\mathbf{u})$, $j = 1, \dots, n_e^k + n_l^k$, be measurable mappings from $\mathcal{U}_k \subseteq \mathbb{R}^{d_u}$ into \mathbb{R} ;
- (iii) $H_{\mathbf{u},j}^k \in \mathbb{R}$, $j = 1, \dots, n_e^k + n_l^k$, be constants;
- (iv) $h_{\mathbf{u},0}^k(\mathbf{u}) := \mathbb{1}_{\mathcal{U}_k}(\mathbf{u})$ and $H_{\mathbf{u},0}^k := 1$.

Find the sequence of cpdfs, $\left\{ \left(\tilde{f}_{\mathbf{U}}^k \right)^* \right\}_{\mathcal{K}} := \{f^*(\mathbf{u}_k|\mathbf{x}_{k-1})\}_{\mathcal{K}}$, such that:

$$\begin{aligned} \left\{ \left(\tilde{f}_{\mathbf{U}}^k \right)^* \right\}_{\mathcal{K}} &\in \arg \min_{\left\{ \tilde{f}_{\mathbf{U}}^k \right\}_{\mathcal{K}}} \mathcal{D}_{KL}(f^n||g^n) \\ \text{s.t.:} \quad c_{\mathbf{u},j}^k \left[\tilde{f}_{\mathbf{U}}^k \right] &= 0, \quad \forall j \in \mathcal{E}_0^k, k \in \mathcal{K} \\ c_{\mathbf{u},j}^k \left[\tilde{f}_{\mathbf{U}}^k \right] &\leq 0, \quad \forall j \in \mathcal{I}^k, k \in \mathcal{K} \end{aligned} \quad (6)$$

where

$$c_{\mathbf{u},j}^k \left[\tilde{f}_{\mathbf{U}}^k \right] := \mathbb{E}_{\tilde{f}_{\mathbf{U}}^k} [h_{\mathbf{u},j}^k(\mathbf{U}_k)] - H_{\mathbf{u},j}^k, \quad (7)$$

and where $\mathcal{E}_0^k := \mathcal{E}^k \cup \{0\}$ (with $\mathcal{E}^k := \{j\}_1^{n_e^k}$), $\mathcal{I}^k :=$

$\{j\}_{n_e^k+1}^{n_e^k+n_l^k}$ are the equality and inequality constraints index sets at time t_k respectively.

As noted in (Pegueroles and Russo, 2019), in the special case when in Problem 1 there are no constraints and the pdfs f^n , g^n are normal distributions with zero mean, then the control policy solving the problem has the same update rules as the Linear Quadratic Regulator. The introduction of the constraints formalized in Problem 1 can be useful in situations of practical interest where the actuation capabilities of the system are different from the actuation capabilities of the demonstrators. Also, by embedding actuation constraints into the problem formulation and by solving the resulting problem, one can *export* the policy that has been synthesized on a given system to other systems having different actuation capabilities. We close this section with the following:

Remark 2 In Problem 1, the constraints are formalized as expectations and can be equivalently written as $\int_{S(\bar{f}_U^k)} \bar{f}_U^k h_{u,j}^k(\mathbf{u}) d\mathbf{u} = H_{u,j}^k$. The equality and inequality constraints, and their number, can change over time. Finally, the first equality constraint is a normalization constraint on the solution of the problem.

4 Technical Results

We now introduce our main technical results. The key result behind the algorithm of Section 5 is Theorem 1. The proof of this theorem, given in this section, makes use of two technical results (i.e. Lemma 1 and Lemma 2). With our first result, i.e. Lemma 1, we tackle an *auxiliary* problem that is iteratively solved within the proof of Theorem 1. This auxiliary problem is formalized next.

Problem 2 Let:

- (i) $\mathcal{Z} \subseteq \mathbb{R}^{d_z}$, \mathcal{F}_z be a σ -algebra on \mathcal{Z} and n_e, n_l be two positive integers;
- (ii) \mathbf{Z} be a random vector on the measurable space $(\mathcal{Z}, \mathcal{F}_z)$;
- (iii) $g := g_{\mathbf{Z}}(\mathbf{z})$ be a pdf over $(\mathcal{Z}, \mathcal{F}_z)$;
- (iv) $\alpha : \mathcal{Z} \mapsto \mathbb{R}$ be a mapping from \mathcal{Z} into \mathbb{R} , which is integrable under the measure given by $f_{\mathbf{Z}}(\mathbf{z})$;
- (v) $\mathbf{z} \mapsto h_j(\mathbf{z})$, $j = 1, \dots, n_e + n_l$, be measurable mappings from \mathcal{Z} into \mathbb{R} ;
- (vi) $H_j \in \mathbb{R}$, $j = 1, \dots, n_e + n_l$, be a constant;
- (vii) $h_0(\mathbf{z}) := \mathbb{1}_{\mathcal{S}(\mathbf{z})}(\mathbf{z})$ and $H_0 := 1$.

Find the pdf $f^* := f_{\mathbf{Z}}^*(\mathbf{z})$ over $(\mathcal{Z}, \mathcal{F}_z)$ such that:

$$\begin{aligned} f^* &\in \arg \min_f \mathcal{L}(f) \\ \text{s.t.: } &c_j[f] = 0, \forall j \in \mathcal{E}_0, \\ &c_j[f] \leq 0, \forall j \in \mathcal{I}, \end{aligned} \quad (8)$$

where:

$$\mathcal{L}(f) := \mathcal{D}_{KL}(f||g) + \int f_{\mathbf{Z}}(\mathbf{z}) \alpha(\mathbf{z}) d\mathbf{z}, \quad (9)$$

with

$$c_j[f] := \int f_{\mathbf{Z}}(\mathbf{z}) h_j(\mathbf{z}) d\mathbf{z} - H_j, \quad (10)$$

and $\mathcal{E}_0 := \mathcal{E} \cup \{0\}$, $\mathcal{E} := \{j\}_1^{n_e}$, $\mathcal{I} := \{j\}_{n_e+1}^{n_e+n_l}$.

We consider feasible sets of constraints that satisfy the following constraint qualification condition (CQC):

Definition 2 Consider the set of linear constraints

$$\begin{cases} c_i[f] = 0, & i = 1, \dots, n_e \\ c_j[f] \leq 0, & j = 1, \dots, n_l. \end{cases}$$

The Slater's CQC (or simply Slater's condition in what follows) is said to hold for such a set if there exists a pdf, say $\bar{f}(\cdot)$, such that $c_i[\bar{f}] = 0$, $\forall i \in \{1, \dots, n_e\}$ and $c_j[\bar{f}] < 0$, $\forall j \in \{1, \dots, n_l\}$.

Remark 3 Slater's condition is also known in the literature on infinite-dimensional optimization problems as a regularity condition on the constraint set (Rockafeller, 1976; Ben-Tal et al., 1988). For a convex infinite-dimensional optimization problem, the fulfillment of such a condition guarantees strong duality (Ben-Tal et al., 1988; Nishiyama, 2020).

We make the following:

Assumption 1 The constraints sets in (6) and in (8) are feasible and satisfy Slater's condition.

Remark 4 Assumption 1 is widely used in the literature on e.g. infinite-dimensional optimization (Ben-Tal et al., 1988; Fan, 1968), divergences optimization (Nishiyama, 2020) and cross-entropy problems (Singh and Vishnoi, 2014; Bot et al., 2005). If the problems involve discrete distributions, then checking feasibility and the Slater's condition implies solving (finite dimensional) systems of equalities and inequalities, see e.g. (Duffin et al., 1956; Fan, 1975; Hiebert, 1980; Censor and Elfving, 1982).

We are now ready to introduce the next result, which gives a solution to Problem 2.

Lemma 1 Consider Problem 2. Then:

(R1) the problem has a unique solution and this is given by the pdf

$$f^* = g \frac{e^{-\left\{ \alpha(\mathbf{z}) + \sum_{j \in \mathcal{A}(f^*) \setminus \{0\}} \lambda_j^* h_j(\mathbf{z}) \right\}}}{e^{1 + \lambda_0^*}}. \quad (11)$$

In (11), λ_j^* is the LM associated to the constraint $c_j[f]$ and $\mathcal{A}(f^*)$ is the active index set defined as

$$\mathcal{A}(f) := \mathcal{E}_0 \cup \{j \in \mathcal{I} : c_j[f] = 0\}. \quad (12)$$

In (11) the LMs $\boldsymbol{\lambda}^* := [\lambda_0^*, \lambda_1^*, \dots, \lambda_{n_e+n_l}^*]^T$ can be computed by solving the optimization problem

$$\begin{aligned} \boldsymbol{\lambda}^* \in \arg \max_{\boldsymbol{\lambda}} \mathcal{L}^D(\boldsymbol{\lambda}) \\ \text{s.t.: } \lambda_j \text{ free, } \forall j \in \mathcal{E}_0 \\ \lambda_j \geq 0, \forall j \in \mathcal{I} \end{aligned} \quad (13)$$

where

$$\begin{aligned} \mathcal{L}^D(\boldsymbol{\lambda}) &:= \\ &= -\langle \boldsymbol{\lambda}, \mathbf{H} \rangle - \int g_{\mathbf{Z}}(\mathbf{z}) e^{-\{1+\alpha(\mathbf{z})+\langle \boldsymbol{\lambda}, \mathbf{h}(\mathbf{z}) \rangle\}} d\mathbf{z}. \end{aligned} \quad (14)$$

(R2) Moreover, the corresponding minimum is

$$\mathcal{L}^* := \mathcal{L}(f^*) = - \left(1 + \sum_{j \in \mathcal{A}(f^*)} \lambda_j^* H_j \right). \quad (15)$$

Proof: See the appendix. \square

Before introducing the next technical result, we make the following remarks on Lemma 1.

Remark 5 The equality constraints in (10) can be used to impose parametric prescriptions on the solution. For example, one could impose that $f_{\mathbf{Z}}^*(\mathbf{z})$ has the central moment of order i equal to some $m_{\mathbf{Z}}^i$. This is equivalent to impose that the solution satisfies $\mathbb{E}_f[\mathbf{Z}^i] = m_{\mathbf{Z}}^i$, which in turn can be formalized as $c_i[f] := \int f_{\mathbf{Z}}(\mathbf{z}) \mathbf{z}^i d\mathbf{z} - m_{\mathbf{Z}}^i$.

Remark 6 The inequality constraints in (10) can also be used to assign properties to the solution: with these constraints, one could express bounds on the expected value of any function of \mathbf{Z} , say $h(\mathbf{Z})$. For instance, the rectangular bound $\underline{m}_{\mathbf{Z}}^2 \leq \mathbb{E}_f[\mathbf{Z}^2] \leq \overline{m}_{\mathbf{Z}}^2$ can be formalized with the pair of inequality constraints:

$$\begin{cases} c_a[f] := \int f_{\mathbf{Z}}(\mathbf{z}) \mathbf{z}^2 d\mathbf{z} - \overline{m}_{\mathbf{Z}}^2 \\ c_b[f] := \int f_{\mathbf{Z}}(\mathbf{z}) (-\mathbf{z}^2) d\mathbf{z} + \underline{m}_{\mathbf{Z}}^2. \end{cases}$$

Remark 7 The LM λ_0 in (11) can be expressed as a function of all the other LMs. This can be done by imposing the normalization constraint, i.e. $c_0[f^*] = 0$, on

the pdf solving the problem, i.e. (11). This yields:

$$\begin{aligned} 1 + \lambda_0 &= \\ &= \ln \left(\int g_{\mathbf{Z}}(\mathbf{z}) e^{-\left\{ \alpha(\mathbf{z}) + \sum_{j \in \mathcal{A}(f^*) \setminus \{0\}} \lambda_j h_j(\mathbf{z}) \right\}} d\mathbf{z} \right). \end{aligned} \quad (16)$$

Condition (16) can also be obtained by imposing the stationarity condition of the Lagrange dual function with respect to λ_0 . The expression for λ_0 in (16) could be directly embedded in the dual cost function (14), yielding

$$\begin{aligned} \mathcal{L}^D(\boldsymbol{\lambda}) &= \\ &= - \sum_{j \in \mathcal{E} \cup \mathcal{I}} \lambda_j H_j + \\ &\quad - \ln \left(\int g_{\mathbf{Z}}(\mathbf{z}) e^{-\left\{ \alpha(\mathbf{z}) + \sum_{j \in \mathcal{E} \cup \mathcal{I}} \lambda_j h_j(\mathbf{z}) \right\}} d\mathbf{z} \right), \end{aligned}$$

and thus reducing by one the dimension of the search space of the dual problem.

We now introduce the following technical result that is also used in the proof of Theorem 1.

Lemma 2 Let f^n and g^n be the pdfs defined in (3) and (5), respectively. Then:

$$\begin{aligned} \mathcal{D}_{KL}(f^n || g^n) &= \\ &= \mathcal{D}_{KL}(f^{n-1} || g^{n-1}) + \mathbb{E}_{f^{n-1}} \left[\mathcal{D}_{KL}(\tilde{f}^n || \tilde{g}^n) \right]. \end{aligned} \quad (17)$$

Proof: The result is obtained from Property 1 (see the appendix for a proof of this property) by setting $\mathbf{Y} := [\mathbf{X}_0, \mathbf{U}_1, \mathbf{X}_1, \dots, \mathbf{U}_{n-1}, \mathbf{X}_{n-1}]$ and $\mathbf{Z} := [\mathbf{U}_n, \mathbf{X}_n]$. \square

The main result behind the algorithm of Section 5, the proof of which makes use of the above technical results, is presented next.

Theorem 1 Consider Problem 1. Then:

(R1) The control policy at time instant t_k , say $\left(\tilde{f}_{\mathbf{U}}^k\right)^* := f^*(\mathbf{u}_k | \mathbf{x}_{k-1})$, composing the sequence of cpdfs $\left\{ \left(\tilde{f}_{\mathbf{U}}^k\right)^* \right\}_{\kappa}$ solving the problem is given by

$$\left(\tilde{f}_{\mathbf{U}}^k\right)^* = \tilde{g}_{\mathbf{U}}^k \frac{e^{-\{\hat{\omega}(\mathbf{u}_k, \mathbf{x}_{k-1}) + \sum_{j \in \mathcal{A}^k \setminus \{0\}} (\lambda_{\mathbf{u},j}^k)^* h_{\mathbf{u},j}^k(\mathbf{u}_k)\}}}{e^{1+(\lambda_{\mathbf{u},0}^k)^*}}, \quad (18)$$

where:

- $\hat{\omega}(\cdot, \cdot)$ is generated via the backward recursion

$$\hat{\omega}(\mathbf{u}_k, \mathbf{x}_{k-1}) = \hat{\alpha}(\mathbf{u}_k, \mathbf{x}_{k-1}) + \hat{\beta}(\mathbf{u}_k, \mathbf{x}_{k-1}), \quad (19)$$

with

$$\begin{aligned}\hat{\alpha}(\mathbf{u}_k, \mathbf{x}_{k-1}) &:= \mathcal{D}_{KL}(\tilde{f}_{\mathbf{X}}^k || \tilde{g}_{\mathbf{X}}^k) \\ \hat{\beta}(\mathbf{u}_k, \mathbf{x}_{k-1}) &:= -\mathbb{E}_{\tilde{f}_{\mathbf{X}}^k}[\ln \hat{\gamma}(\mathbf{X}_k)],\end{aligned}\quad (20)$$

and terminal conditions $\hat{\beta}(\mathbf{u}_n, \mathbf{x}_{n-1}) = 0, \hat{\alpha}(\mathbf{u}_n, \mathbf{x}_{n-1}) = \mathcal{D}_{KL}(\tilde{f}_{\mathbf{X}}^n || \tilde{g}_{\mathbf{X}}^n)$;

- $\hat{\gamma}(\cdot)$ in (20) is defined as

$$\ln \hat{\gamma}(\mathbf{x}_{k-1}) := \left[\sum_{j \in \mathcal{A}^k} \ln(\hat{\gamma}_{\mathbf{u},j}^k(\mathbf{x}_{k-1})) \right], \quad (21)$$

with

$$\hat{\gamma}_{\mathbf{u},0}^k(\mathbf{x}_{k-1}) = \exp\{(\lambda_{\mathbf{u},0}^k)^* + 1\}, \quad \hat{\gamma}_{\mathbf{u},0}^{n+1}(\mathbf{x}_n) = 1, \quad (22)$$

and

$$\hat{\gamma}_{\mathbf{u},j}^k(\mathbf{x}_{k-1}) := \exp\{(\lambda_{\mathbf{u},j}^k)^* H_{\mathbf{u},j}^k\}, \quad \hat{\gamma}_{\mathbf{u},j}^{n+1}(\mathbf{x}_n) = 1, \quad (23)$$

$\forall j \in \mathcal{E}^k \cup \mathcal{I}^k$;

- $(\lambda_{\mathbf{u},j}^k)^*$ in (18) is the Lagrange multiplier associated to the constraint $c_{\mathbf{u},j}^k$, while \mathcal{A}^k is the active index set associated to $(\tilde{f}_{\mathbf{U}}^k)^*$. In particular, the vector of LMs $(\lambda_{\mathbf{u}}^k)^* := [(\lambda_{\mathbf{u},0}^k)^*, (\lambda_{\mathbf{u},1}^k)^*, \dots, (\lambda_{\mathbf{u},n_e^k+n_t^k}^k)^*]^T$ can be computed solving:

$$\begin{aligned}(\lambda_{\mathbf{u}}^k)^* &\in \arg \max_{\lambda_{\mathbf{u}}^k} \mathcal{L}^D(\lambda_{\mathbf{u}}^k) \\ \text{s.t.: } &\lambda_{\mathbf{u},j}^k \text{ free, } \forall j \in \mathcal{E}^k \\ &\lambda_{\mathbf{u},j}^k \geq 0, \forall j \in \mathcal{I}^k\end{aligned}\quad (24)$$

where

$$\begin{aligned}\mathcal{L}^D(\lambda_{\mathbf{u}}^k) &= -\sum_{j \in \mathcal{E}^k \cup \mathcal{I}^k} \lambda_{\mathbf{u},j}^k H_{\mathbf{u},j}^k + \\ &\quad -\ln \left(\int \tilde{g}_{\mathbf{U}}^k e^{-\hat{\omega}(\mathbf{u}_k, \mathbf{x}_{k-1})} \right. \\ &\quad \left. e^{-\left\{ \sum_{j \in \mathcal{E}^k \cup \mathcal{I}^k} \lambda_{\mathbf{u},j}^k h_{\mathbf{u},j}^k(\mathbf{u}_k) \right\}} d\mathbf{u}_k \right),\end{aligned}$$

with $(\lambda_{\mathbf{u},0}^k)^*$ given by

$$\begin{aligned}(\lambda_{\mathbf{u},0}^k)^* &= \\ &= \ln \left(\int \tilde{g}_{\mathbf{U}}^k e^{-\hat{\omega}(\mathbf{u}_k, \mathbf{x}_{k-1})} \right. \\ &\quad \left. e^{-\left\{ \sum_{j \in \mathcal{A}^k \setminus \{0\}} (\lambda_{\mathbf{u},j}^k)^* h_{\mathbf{u},j}^k(\mathbf{u}_k) \right\}} d\mathbf{u}_k \right) - 1.\end{aligned}\quad (25)$$

(R2) Moreover, the corresponding minimum at time t_k is given by:

$$B_k^* := -\mathbb{E}_{p_{\mathbf{X}}^{k-1}}[\ln \hat{\gamma}(\mathbf{X}_{k-1})]. \quad (26)$$

where $p_{\mathbf{X}}^k$ denotes the pdf of the state at time t_k (i.e. $p_{\mathbf{X}}^k := f(\mathbf{x}_k)$).

Before introducing the proof we make the following:

Remark 8 The policy solving Problem 1, i.e. $(f_{\mathbf{U}}^k)^*$, directly depends on $g_{\mathbf{U}}^k$. This is the policy extracted from the examples and a natural choice is to estimate it from the data (see also the example in Section 5). In principle, one could use an arbitrary $g_{\mathbf{U}}^k$ that, while not being extracted from the examples, embeds design preferences that might be known a-priori. Another choice, for pdfs having compact supports, is to set $g_{\mathbf{U}}^k$ equal to the uniform distribution. In this case, it can be shown that solving Problem 1 is equivalent to maximizing Shannon's entropy.

Proof: We prove the result by induction and the proof is organized in steps. First, in **Step 1**, we leverage Lemma 2 to show that Problem 1 can be split into sub-problems, where the optimization sub-problem for the last iteration, i.e. $k = n$, can be solved independently on the others. We then (**Step 2**) make use of Lemma 1 to find an explicit solution for the sub-problem at $k = n$. Once this is done, we update the cost function of Problem 1 with the minimum found by solving the sub-problem at $k = n$ and show, in **Step 3**, that the original problem can be again broken down into sub-problems. This time, the sub-problem at iteration $k = n - 1$ can be solved independently on the others. We then solve this sub-problem and note, in **Step 4**, how $\forall k = 1, \dots, n - 2$ the structure of the optimization remains the same. From this, the desired conclusions are drawn.

Before proceeding with the proof note that, for notational convenience, we use the shorthand notation $\{\mathbf{C}_{\mathbf{u}}^k\}$ to denote the set of constraints of Problem 1 at iteration k . We also denote by $\{\mathbf{C}_{\mathbf{u}}^k\}_{\mathcal{K}}$ the set of constraints over the whole time horizon \mathcal{K} and $\{\mathbf{C}_{\mathbf{u}}^k\}_{k=1}^{n-1}$ to denote the constraints from t_1 up to iteration $n - 1$.

Step 1. Note that, following Lemma 2, Problem 1 can be re-written as

$$\begin{aligned}&\min_{\{\tilde{f}_{\mathbf{U}}^k\}_{\mathcal{K}}} \mathcal{D}_{KL}(f^n || g^n) = \\ &\text{s.t.: } \{\mathbf{C}_{\mathbf{u}}^k\}_{\mathcal{K}} \\ &= \min_{\{\tilde{f}_{\mathbf{U}}^k\}_{k=1}^{n-1}} \{ \mathcal{D}_{KL}(f^{n-1} || g^{n-1}) + B_n^* \} \\ &\text{s.t.: } \{\mathbf{C}_{\mathbf{u}}^k\}_{k=1}^{n-1}.\end{aligned}\quad (27)$$

where:

$$B_n^* := \min_{\tilde{f}_{\mathbf{U}}^n} B_n \quad (28a)$$

$$\text{s.t.: } \mathbf{C}_{\mathbf{u}}^n,$$

and

$$B_n := \mathbb{E}_{f^{n-1}} \left[\mathcal{D}_{\text{KL}} \left(\tilde{f}^n \parallel \tilde{g}^n \right) \right]. \quad (28b)$$

That is, Problem 1 can be approached by solving first the optimization of the last iteration of the horizon \mathcal{K} (the term B_n in (27)) and then by taking into account the result from this optimization problem in the optimization up to iteration $n-1$.

Step 2. We first observe that, for B_n defined in (28a):

$$B_n = \mathbb{E}_{f^{n-1}} \left[\mathcal{D}_{\text{KL}} \left(\tilde{f}^n \parallel \tilde{g}^n \right) \right] = \mathbb{E}_{p_{\mathbf{X}}^{n-1}} \left[\mathcal{D}_{\text{KL}} \left(\tilde{f}^n \parallel \tilde{g}^n \right) \right].$$

The above expression was obtained by noticing that $\mathcal{D}_{\text{KL}} \left(\tilde{f}^n \parallel \tilde{g}^n \right)$ is only a function of the previous state and, to stress this in the notation, we let $\hat{A}(\cdot) := \mathcal{D}_{\text{KL}} \left(\tilde{f}^n \parallel \tilde{g}^n \right)$. Hence, B_n can be written as

$$B_n = \mathbb{E}_{p_{\mathbf{X}}^{n-1}} \left[\mathcal{D}_{\text{KL}} \left(\tilde{f}^n \parallel \tilde{g}^n \right) \right] = \mathbb{E}_{p_{\mathbf{X}}^{n-1}} \left[\hat{A}(\mathbf{X}_{n-1}) \right], \quad (29)$$

and the sub-problem in (28a) becomes:

$$B_n^* = \min_{\tilde{f}_{\mathbf{U}}^n} \mathbb{E}_{p_{\mathbf{X}}^{n-1}} \left[\hat{A}(\mathbf{X}_{n-1}) \right] \quad (30)$$

$$\text{s.t.: } \mathbf{C}_{\mathbf{u}}^n.$$

Now, note that

$$\min_{\tilde{f}_{\mathbf{U}}^n} \mathbb{E}_{p_{\mathbf{X}}^{n-1}} \left[\hat{A}(\mathbf{X}_{n-1}) \right] = \mathbb{E}_{p_{\mathbf{X}}^{n-1}} [A_n^*], \quad (31)$$

$$\text{s.t.: } \mathbf{C}_{\mathbf{u}}^n$$

where

$$A_n^* := \min_{\tilde{f}_{\mathbf{u}}^n} \hat{A}(\mathbf{x}_{n-1}) \quad (32)$$

$$\text{s.t.: } \mathbf{C}_{\mathbf{u}}^n.$$

Also, the equality in (31) was obtained by using the fact that the expectation operator is linear and the fact that the decision variable (i.e. $\tilde{f}_{\mathbf{U}}^n$) is independent on the pdf over which the expectation is performed (i.e. $p_{\mathbf{X}}^{n-1}$).

Following (31), we can obtain B_n^* by solving (32) and then by averaging A_n^* over $p_{\mathbf{X}}^{n-1}$. We now focus on solving problem (32). From (29), we get:

$$\hat{A}(\mathbf{x}_{n-1}) = \int \tilde{f}_{\mathbf{U}}^n \left[\ln \left(\frac{\tilde{f}_{\mathbf{U}}^n}{\tilde{g}_{\mathbf{U}}^n} \right) + \hat{\alpha}(\mathbf{u}_n, \mathbf{x}_{n-1}) \right] d\mathbf{u}_n, \quad (33a)$$

$$\hat{\alpha}(\mathbf{u}_n, \mathbf{x}_{n-1}) := \mathcal{D}_{\text{KL}} \left(\tilde{f}_{\mathbf{X}}^n \parallel \tilde{g}_{\mathbf{X}}^n \right). \quad (33b)$$

In turn, (33a) can be compactly written as:

$$\hat{A}(\mathbf{x}_{n-1}) = \mathcal{D}_{\text{KL}} \left(\tilde{f}_{\mathbf{U}}^n \parallel \tilde{g}_{\mathbf{U}}^n \right) + \int \tilde{f}_{\mathbf{U}}^n \hat{\alpha}(\mathbf{u}_n, \mathbf{x}_{n-1}) d\mathbf{u}_n,$$

where we used the definition of KL-divergence.

Hence, Lemma 1 can be used to solve the optimization problem in (32). Indeed by applying Lemma 1 with: $\mathbf{Z} = \mathbf{U}_n$, $f = \tilde{f}_{\mathbf{U}}^n$, $g = \tilde{g}_{\mathbf{U}}^n$, $\alpha(\cdot) = \hat{\alpha}(\cdot, \mathbf{x}_{n-1})$, $h_j = h_{\mathbf{u},j}^n$, $H_j = H_{\mathbf{u},j}^n$, $c_j = c_{\mathbf{u},j}^n$, $\lambda_j = \lambda_{\mathbf{u},j}^n$, $\mathcal{E} = \mathcal{E}^n$, $\mathcal{I} = \mathcal{I}^n$, we get the following solution to (32):

$$\left(\tilde{f}_{\mathbf{U}}^n \right)^* = \tilde{g}_{\mathbf{U}}^n \frac{e^{-\{\hat{\alpha}(\mathbf{u}_n, \mathbf{x}_{n-1}) + \sum_{j \in \mathcal{A}^n \setminus \{0\}} (\lambda_{\mathbf{u},j}^n)^* h_{\mathbf{u},j}^n(\mathbf{u}_n)\}}}{e^{1 + (\lambda_{\mathbf{u},0}^n)^*}}, \quad (34)$$

where \mathcal{A}^n is the active set index associated to $\left(\tilde{f}_{\mathbf{U}}^n \right)^*$.

In the above pdf, $(\lambda_{\mathbf{u},j}^n)^*$, $j \in \mathcal{E}_0^n \cup \mathcal{I}^n$ are the LMs at the last iteration $k = n$. Now, following Lemma 1 and Remark 7, the LMs $(\lambda_{\mathbf{u}}^n)^* = [(\lambda_{\mathbf{u},0}^n)^*, (\lambda_{\mathbf{u},1}^n)^*, \dots, (\lambda_{\mathbf{u},n_e^n + n_l^n}^n)^*]^T$ are computed by solving

$$(\lambda_{\mathbf{u}}^n)^* \in \arg \max \mathcal{L}^D(\lambda_{\mathbf{u}}^n)$$

$$\text{s.t.: } \lambda_{\mathbf{u},j}^n \text{ free, } \forall j \in \mathcal{E}^n,$$

$$\lambda_{\mathbf{u},j}^n \geq 0, \forall j \in \mathcal{I}^n,$$

choosing $[(\lambda_{\mathbf{u},1}^n)^*, \dots, (\lambda_{\mathbf{u},n_e^n + n_l^n}^n)^*]^T$ so that $\left(\tilde{f}_{\mathbf{U}}^n \right)^*$ is feasible. In the above expression

$$\mathcal{L}^D(\lambda_{\mathbf{u}}^n) = - \sum_{j \in \mathcal{E}^n \cup \mathcal{I}^n} \lambda_{\mathbf{u},j}^n H_{\mathbf{u},j}^n +$$

$$- \ln \left(\int \tilde{g}_{\mathbf{U}}^n e^{-\hat{\alpha}(\mathbf{u}_n, \mathbf{x}_{n-1})} \right.$$

$$\left. e^{-\left\{ \sum_{j \in \mathcal{E}^n \cup \mathcal{I}^n} \lambda_{\mathbf{u},j}^n h_{\mathbf{u},j}^n(\mathbf{z}) \right\}} d\mathbf{u}_n \right),$$

and $(\lambda_{\mathbf{u},0}^n)^*$ can be obtained from all the other LMs by normalizing (34), i.e.:

$$(\lambda_{\mathbf{u},0}^n)^* + 1 = \ln \left(\int \tilde{g}_{\mathbf{U}}^n e^{-\hat{\alpha}(\mathbf{u}_n, \mathbf{x}_{n-1})} \right.$$

$$\left. e^{-\left\{ \sum_{j \in \mathcal{A}^n \setminus \{0\}} (\lambda_{\mathbf{u},j}^n)^* h_{\mathbf{u},j}^n(\mathbf{u}_n) \right\}} d\mathbf{u}_n \right)$$

$$= \ln \left(\hat{\gamma}_{\mathbf{u},0}^n(\mathbf{x}_{n-1}) \right).$$

Moreover, from Lemma 1, the minimum of the problem

in (32) is given by:

$$\hat{A}_n^* = - \left(1 + \sum_{j \in \mathcal{A}^n} (\lambda_{\mathbf{u},j}^n)^* H_{\mathbf{u},j}^n \right),$$

which, using the definitions in (22) and (23), can be equivalently written as

$$\hat{A}_n^* = - \left[\sum_{j \in \mathcal{A}^n} \ln (\hat{\gamma}_{\mathbf{u},j}^n (\mathbf{x}_{n-1})) \right] = - \ln \hat{\gamma} (\mathbf{x}_{n-1}).$$

Thus, we get:

$$B_n^* = -\mathbb{E}_{p_{\mathbf{x}}^{n-1}} [\ln \hat{\gamma} (\mathbf{X}_{n-1})]. \quad (35)$$

Step 3. Note now that the B_n^* in (35) only depends on \mathbf{X}_{n-1} and therefore the original problem (27) can be split, following Lemma 2, as

$$\begin{aligned} \min_{\{\tilde{f}_{\mathbf{U}}^k\}_{k=1}^{n-1}} \{ \mathcal{D}_{\text{KL}} (f^{n-1} || g^{n-1}) + B_n^* \} = \\ \text{s.t.: } \{ \mathbf{C}_{\mathbf{u}}^k \}_{k=1}^{n-1} \\ = \min_{\{\tilde{f}_{\mathbf{U}}^k\}_{k=1}^{n-2}} \{ \mathcal{D}_{\text{KL}} (f^{n-2} || g^{n-2}) + B_{n-1}^* \} \\ \text{s.t.: } \{ \mathbf{C}_{\mathbf{u}}^k \}_{k=1}^{n-2}, \end{aligned} \quad (36)$$

where:

$$\begin{aligned} B_{n-1}^* &:= \min_{\tilde{f}_{\mathbf{U}}^{n-1}} B_{n-1} \\ \text{s.t.: } &\mathbf{C}_{\mathbf{u}}^{n-1}, \end{aligned} \quad (37a)$$

$$B_{n-1} := \mathbb{E}_{f^{n-2}} \left[\mathcal{D}_{\text{KL}} (\tilde{f}^{n-1} || \tilde{g}^{n-1}) \right] + B_n^*. \quad (37b)$$

We approach the above problem in the same way we used to solve the problem in (30). We do this by finding a function, $\hat{A}(\mathbf{x}_{n-2})$, such that $B_{n-1} = \mathbb{E}_{p_{\mathbf{x}}^{n-2}} [\hat{A}(\mathbf{X}_{n-2})]$. Once this is done, we then get

$$\begin{aligned} A_{n-1}^* &:= \min_{\tilde{f}_{\mathbf{U}}^{n-1}} \hat{A}(\mathbf{x}_{n-2}) \\ \text{s.t.: } &\mathbf{C}_{\mathbf{u}}^{n-1}, \end{aligned} \quad (38)$$

and obtain B_{n-1}^* as $B_{n-1}^* := \mathbb{E}_{p_{\mathbf{x}}^{n-2}} [A_{n-1}^*]$. To this end we first note that the following identities

$$\mathbb{E}_{p_{\mathbf{x}}^{n-1}} [\varphi(\mathbf{X}_{n-1})] = \mathbb{E}_{p_{\mathbf{x}}^{n-2}} [\mathbb{E}_{\tilde{f}^{n-1}} [\varphi(\mathbf{X}_{n-1})]] \quad (39a)$$

$$\mathbb{E}_{\tilde{f}_{\mathbf{x}}^{n-1}} [\varphi(\mathbf{X}_{n-1})] = \mathbb{E}_{\tilde{f}_{\mathbf{x}}^{n-2}} [\mathbb{E}_{\tilde{f}^{n-1}} [\varphi(\mathbf{X}_{n-1})]] \quad (39b)$$

hold for any function φ of \mathbf{X}_{n-1} . Therefore, by means of (35) and (39a) we obtain, from (37b):

$$\begin{aligned} B_{n-1} &= \\ &= \mathbb{E}_{f^{n-2}} \left[\mathcal{D}_{\text{KL}} (\tilde{f}^{n-1} || \tilde{g}^{n-1}) \right] + B_n^* \\ &= \mathbb{E}_{p_{\mathbf{x}}^{n-2}} \left[\mathcal{D}_{\text{KL}} (\tilde{f}^{n-1} || \tilde{g}^{n-1}) \right] + B_n^* \\ &= \mathbb{E}_{p_{\mathbf{x}}^{n-2}} \left[\mathcal{D}_{\text{KL}} (\tilde{f}^{n-1} || \tilde{g}^{n-1}) \right] + \\ &\quad - \mathbb{E}_{p_{\mathbf{x}}^{n-2}} \left[\mathbb{E}_{\tilde{f}^{n-1}} [\ln \hat{\gamma} (\mathbf{X}_{n-1})] \right] \\ &= \mathbb{E}_{p_{\mathbf{x}}^{n-2}} \left[\underbrace{\mathcal{D}_{\text{KL}} (\tilde{f}^{n-1} || \tilde{g}^{n-1}) + \mathbb{E}_{\tilde{f}^{n-1}} [-\ln \hat{\gamma} (\mathbf{X}_{n-1})]}_{=: \hat{A}(\mathbf{X}_{n-2})} \right], \end{aligned}$$

and the term $\hat{A}(\mathbf{x}_{n-2})$ can hence be recognized. Now, following the same reasoning we used to obtain $\hat{A}(\mathbf{x}_{n-1})$, we explicitly write $\hat{A}(\mathbf{x}_{n-2})$ in compact form as

$$\begin{aligned} \hat{A}(\mathbf{x}_{n-2}) &= \mathcal{D}_{\text{KL}} (\tilde{f}^{n-1} || \tilde{g}^{n-1}) + \mathbb{E}_{\tilde{f}_{\mathbf{U}}^{n-1}} \left[\mathbb{E}_{\tilde{f}_{\mathbf{x}}^{n-1}} [-\ln \hat{\gamma} (\mathbf{X}_{n-1})] \right] = \\ &= \int \tilde{f}_{\mathbf{U}}^{n-1} \left\{ \ln \left(\frac{\tilde{f}_{\mathbf{U}}^{n-1}}{\tilde{g}_{\mathbf{U}}^{n-1}} \right) + \hat{\omega}(\mathbf{u}_{n-1}, \mathbf{x}_{n-2}) \right\} d\mathbf{u}_{n-1}, \end{aligned} \quad (40)$$

where $\hat{\omega}(\mathbf{u}_{n-1}, \mathbf{x}_{n-2}) = \hat{\alpha}(\mathbf{u}_{n-1}, \mathbf{x}_{n-2}) + \hat{\beta}(\mathbf{u}_{n-1}, \mathbf{x}_{n-2})$ and

$$\begin{aligned} \hat{\alpha}(\mathbf{u}_{n-1}, \mathbf{x}_{n-2}) &:= \mathcal{D}_{\text{KL}} (\tilde{f}_{\mathbf{x}}^{n-1} || \tilde{g}_{\mathbf{x}}^{n-1}) \\ \hat{\beta}(\mathbf{u}_{n-1}, \mathbf{x}_{n-2}) &:= -\mathbb{E}_{\tilde{f}_{\mathbf{x}}^{n-1}} [\ln \hat{\gamma} (\mathbf{X}_{n-1})]. \end{aligned}$$

The last expression we found for $\hat{A}(\mathbf{x}_{n-2})$ in (40) enables us to use Lemma 1 in order to solve the optimization problem in (38). This time, by applying Lemma 1 with $\mathbf{Z} = \mathbf{U}_{n-1}$, $f = \tilde{f}_{\mathbf{U}}^{n-1}$, $g = \tilde{g}_{\mathbf{U}}^{n-1}$, $\alpha(\cdot) = \hat{\omega}(\cdot, \mathbf{x}_{n-2})$, $h_j = h_{\mathbf{u},j}^{n-1}$, $H_j = H_{\mathbf{u},j}^{n-1}$, $c_j = c_{\mathbf{u},j}^{n-1}$, $\lambda_j = \lambda_{\mathbf{u},j}^{n-1}$, $\mathcal{E} = \mathcal{E}^{n-1}$, $\mathcal{I} = \mathcal{I}^{n-1}$, we get the following solution to (38):

$$\begin{aligned} (\tilde{f}_{\mathbf{U}}^{n-1})^* &= \\ \tilde{g}_{\mathbf{U}}^{n-1} e^{\frac{-\{\hat{\omega}(\mathbf{u}_{n-1}, \mathbf{x}_{n-2}) + \sum_{j \in \mathcal{A}^{n-1} \setminus \{0\}} (\lambda_{\mathbf{u},j}^{n-1})^* h_{\mathbf{u},j}^{n-1}(\mathbf{u}_{n-1})\}}{e^{1+(\lambda_{\mathbf{u},0}^{n-1})^*}}}, \end{aligned}$$

where \mathcal{A}^{n-1} is the active set index associated to $(\tilde{f}_{\mathbf{U}}^{n-1})^*$ and the LMs can again be obtained from Lemma 1. Namely:

$$\bullet (\lambda_{\mathbf{u}}^{n-1})^* = [(\lambda_{\mathbf{u},0}^{n-1})^*, (\lambda_{\mathbf{u},1}^{n-1})^*, \dots, (\lambda_{\mathbf{u},n_{\mathbf{e}}^{n-1}+n_l^n}^{n-1})^*]^T$$

are the solution to

$$\begin{aligned} (\lambda_{\mathbf{u}}^{n-1})^* &\in \arg \max \mathcal{L}^D(\lambda_{\mathbf{u}}^{n-1}) \\ \text{s.t.: } &\lambda_{\mathbf{u},j}^{n-1} \text{ free, } \forall j \in \mathcal{E}^{n-1}, \\ &\lambda_{\mathbf{u},j}^{n-1} \geq 0, \forall j \in \mathcal{I}^{n-1}, \end{aligned}$$

where

$$\begin{aligned} \mathcal{L}^D(\lambda_{\mathbf{u}}^{n-1}) &= -\sum_{j \in \mathcal{E}^{n-1} \cup \mathcal{I}^{n-1}} \lambda_{\mathbf{u},j}^{n-1} H_{\mathbf{u},j}^{n-1} \\ &\quad - \ln \left(\int \tilde{g}_{\mathbf{U}}^{n-1} e^{-\hat{\omega}(\mathbf{u}_{n-1}, \mathbf{x}_{n-2}) +} \right. \\ &\quad \left. e^{-\left\{ \sum_{j \in \mathcal{E}^{n-1} \cup \mathcal{I}^{n-1}} \lambda_{\mathbf{u},j}^{n-1} h_{\mathbf{u},j}^{n-1}(\mathbf{u}_{n-1}) \right\}} d\mathbf{u}_{n-1} \right); \end{aligned}$$

- $(\lambda_{\mathbf{u},0}^{n-1})^*$ is given by

$$\begin{aligned} (\lambda_{\mathbf{u},0}^{n-1})^* + 1 &= \ln \left\{ \int \tilde{g}_{\mathbf{U}}^{n-1} e^{-\{\hat{\omega}(\mathbf{u}_{n-1}, \mathbf{x}_{n-2})\}} \right. \\ &\quad \left. e^{-\left\{ \sum_{j \in \mathcal{A}^{n-1} \setminus \{0\}} (\lambda_{\mathbf{u},j}^{n-1})^* h_{\mathbf{u},j}^{n-1}(\mathbf{u}_{n-1}) \right\}} d\mathbf{u}_{n-1} \right\} \\ &= \ln \{ \hat{\gamma}_{\mathbf{u},0}^{n-1}(\mathbf{x}_{n-2}) \}. \end{aligned}$$

Moreover, from Lemma 1 we also obtain:

$$\begin{aligned} B_{n-1}^* &= -\mathbb{E}_{\tilde{f}_{\mathbf{X}}^{n-2}} \left[\sum_{j \in \mathcal{A}^{n-1}} \ln \hat{\gamma}_{\mathbf{u},j}^{n-1}(\mathbf{X}_{n-2}) \right] \\ &= -\mathbb{E}_{\tilde{f}_{\mathbf{X}}^{n-2}} [\ln \hat{\gamma}(\mathbf{X}_{n-2})]. \end{aligned}$$

Step 4. The proof can then be concluded by observing that, using B_{n-1}^* in (36), the optimization can again be split in sub-problems, with the *last* sub-problem (i.e. the sub-problem corresponding to $k = n - 2$) being independent from the others and having the same structure as the problem we solved at $k = n - 1$. Hence, the solution at the generic iteration k , i.e. $(\tilde{f}_{\mathbf{U}}^k)^*$, will have the same structure as $(\tilde{f}_{\mathbf{U}}^{n-1})^*$, with the functions $\hat{\alpha}(\cdot, \cdot)$, $\hat{\beta}(\cdot, \cdot)$, $\hat{\omega}(\cdot)$ given by (19) - (20) and the LMs given by (24) - (25). This leads to the expression in (18) with the minimum given in (26). Finally, for the last iteration ($k = n$) we note from (33b) that $\hat{\beta}(\mathbf{u}_n, \mathbf{x}_{n-1}) = 0$ which, by means of (21), implies that $\hat{\gamma}_{\mathbf{u},j}^{n+1}(\mathbf{x}_n) = 1, \forall j$. This gives the terminal conditions in (22) and (23). The proof is then completed. \square

5 An algorithm from Theorem 1

Theorem 1 gives an explicit expression for synthesizing the control policy and we leverage this to turn the result into an algorithmic procedure. The algorithm introduced here takes as input $g(\mathbf{d}_e^n)$, $\tilde{f}_{\mathbf{X}}^k := f(\mathbf{x}_k | \mathbf{u}_k, \mathbf{x}_{k-1})$ and

the constraints of Problem 1 (if any). The pdfs, as further illustrated in the next section, can be obtained from the data. Given this input, the algorithm outputs the sequence $\left\{ (\tilde{f}_{\mathbf{U}}^k)^* \right\}_{k \in \mathcal{K}}$ solving Problem 1. The key steps of the proposed algorithm are summarized as pseudo-code in Algorithm 1.

Algorithm 1 Pseudo-code

Inputs:

$g(\mathbf{d}_e^n)$, $\tilde{f}_{\mathbf{X}}^k$ and constraints of Problem 1

Output:

$\left\{ (\tilde{f}_{\mathbf{U}}^k)^* \right\}_{k \in \mathcal{K}}$ solving Problem 1

Initialize

$\hat{\gamma}_{\mathbf{u},j}^{n+1}(\mathbf{x}_n) = 1, \forall j$;

$\hat{\gamma}(\mathbf{x}_n) \leftarrow \exp \left[\sum_j \ln (\hat{\gamma}_{\mathbf{u},j}^{n+1}(\mathbf{x}_n)) \right]$;

for $k = n$ to 1 **do**

$\hat{\alpha}(\mathbf{u}_k, \mathbf{x}_{k-1}) \leftarrow \int f(\mathbf{x}_k | \mathbf{u}_k, \mathbf{x}_{k-1}) \ln \frac{f(\mathbf{x}_k | \mathbf{u}_k, \mathbf{x}_{k-1})}{g(\mathbf{x}_k | \mathbf{u}_k, \mathbf{x}_{k-1})} d\mathbf{x}_k$;

$\hat{\beta}(\mathbf{u}_k, \mathbf{x}_{k-1}) \leftarrow \int f(\mathbf{x}_k | \mathbf{u}_k, \mathbf{x}_{k-1}) \{ -\ln (\hat{\gamma}(\mathbf{x}_k)) \}$;

$\hat{\omega}(\mathbf{u}_k, \mathbf{x}_{k-1}) \leftarrow \hat{\alpha}(\mathbf{u}_k, \mathbf{x}_{k-1}) + \hat{\beta}(\mathbf{u}_k, \mathbf{x}_{k-1})$;

Compute $\left[(\lambda_{\mathbf{u},1}^k)^*, \dots, (\lambda_{\mathbf{u},n_e^k+n_l^k}^k)^* \right]^T$ by solving

(24) and $(\lambda_{\mathbf{u},0}^k)^*$ using (25);

Compute the control policy:

$$(\tilde{f}_{\mathbf{U}}^k)^* \leftarrow \tilde{g}_{\mathbf{U}}^k e^{-\{\hat{\omega}(\mathbf{u}_k, \mathbf{x}_{k-1}) + \sum_{j \in \mathcal{A}^k \setminus \{0\}} (\lambda_{\mathbf{u},j}^k)^* h_{\mathbf{u},j}^k(\mathbf{u}_k)\}} e^{1 + (\lambda_{\mathbf{u},0}^k)^*}; \quad (41)$$

Prepare variables for the next iteration, $k - 1$:

$\hat{\gamma}_{\mathbf{u},0}^k(\mathbf{x}_{k-1}) \leftarrow \exp \{ (\lambda_{\mathbf{u},0}^k)^* + 1 \}$

$\hat{\gamma}_{\mathbf{u},j}^k(\mathbf{x}_{k-1}) \leftarrow \exp \{ (\lambda_{\mathbf{u},j}^k)^* H_{\mathbf{u},j}^k \} \quad j \in \mathcal{E}^k \cup \mathcal{I}^k$

$\hat{\gamma}(\mathbf{x}_{k-1}) \leftarrow \exp \left[\sum_{j \in \mathcal{A}^k} \ln (\hat{\gamma}_{\mathbf{u},j}^k(\mathbf{x}_{k-1})) \right]$

end for

Algorithm 1 is used to compute the control policy for the example of the next section.

6 Numerical example

We now illustrate the effectiveness of the results via a numerical example where the algorithm of Section 5 is used to synthesize, from data measured during test drives, a policy for the merging of a car on a highway. We first describe the scenario considered and the experimental set-up. Then, we describe the data we collected from the test drives and the process we used to compute the pdfs for Algorithm 1. Finally, we discuss the results.

Scenario description and experimental set-up.

The scenario we considered is schematically illustrated in Figure 1, where a car is merging onto a highway. The stretch of road where our experiments took place is outside University College Dublin (UCD) and the

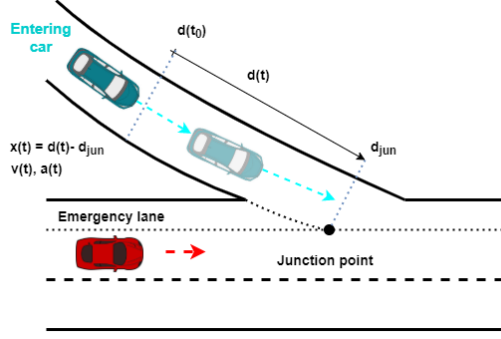


Fig. 1. The scenario considered in Section 6: the light-blue vehicle is trying to merge on a highway.

highway is *Stillorgan Road* in Dublin 4 (see Figure 2). Data were collected from a Toyota Prius using an OBD2² connection with a smartphone running the Android apps *Hybrid Assistant* and its reporting tool *Hybrid Reporter*³. We collected the car GPS position and its longitudinal speed using the hardware-in-the-loop architecture of (Griggs et al., 2019). The apps on the smartphone provided *raw data* in a .txt file with each line reporting the quantities measured at a given time instant (the sampling period was of approximately 0.25s). Data were imported in Matlab and the car position was localized by cross-referencing these data with the road information from *OpenStreetMap* (OpenStreetMap contributors, 2017).

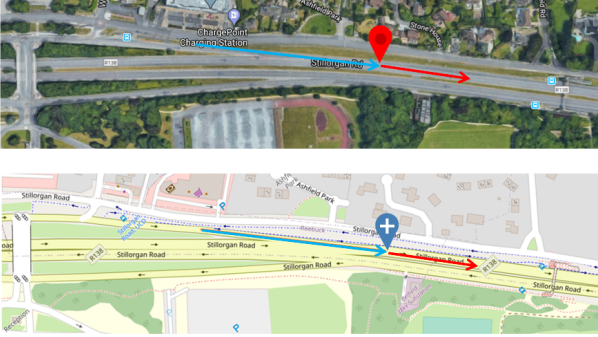


Fig. 2. Area for the experiments: map view (from Google maps) and *OpenStreetMap* representation.

Collecting the data and building the datasets. We performed 100 test drives. In each of the tests, data were collected within a 300 meters observation window starting 200m before the junction (i.e. after the UCD entrance). The raw data were processed to obtain the speed, acceleration and jerk profiles of the car as a function of the distance traveled within the observation window (see left panels in Figure 3). The dataset corre-

sponding to these profiles is termed as *complete* dataset in what follows. The vertical line in each panel highlights the physical location of the junction of Figure 2. From the complete dataset we extracted a subset of profiles that would serve as example dataset. In particular, we selected the profiles with the lowest root mean square (RMS) value for the jerk, which is typically associated to a comfortable driving style, see e.g. (Bae et al., 2019). We used as example driving profiles, those having a RMS value for the jerk of at most 0.16. This gave the subset of 20 driving profiles shown in the right panels of Figure 3.

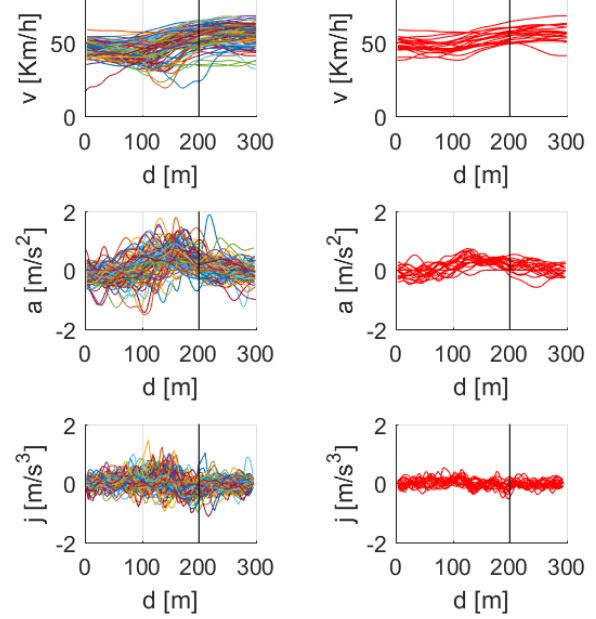


Fig. 3. Left panels: driving profiles from the complete dataset of 100 trips. Right panels: the subset of 20 profiles used as examples. Acceleration and jerk computed from the data.

Computing the pdfs. We let \mathbf{x}_k be the position of the car at the k -th time-step (i.e. $\mathbf{x}_k = d_k$) and \mathbf{u}_k be its longitudinal speed (i.e. $\mathbf{u}_k = v_k$). We first computed the joint probability density functions $f(\mathbf{x}_{k-1}, \mathbf{u}_k)$ and $g(\mathbf{x}_{k-1}, \mathbf{u}_k)$ as the empirical distributions from the complete and the example dataset respectively (see Figure 4). We also estimated from the data $f(\mathbf{x}_k, \mathbf{x}_{k-1}, \mathbf{u}_k)$ and $g(\mathbf{x}_k, \mathbf{x}_{k-1}, \mathbf{u}_k)$ and conditioned these joint pdfs to get $f(\mathbf{x}_k | \mathbf{x}_{k-1}, \mathbf{u}_k) = f(\mathbf{x}_k, \mathbf{x}_{k-1}, \mathbf{u}_k) / f(\mathbf{x}_{k-1}, \mathbf{u}_k)$ and $g(\mathbf{x}_k | \mathbf{x}_{k-1}, \mathbf{u}_k) = g(\mathbf{x}_k, \mathbf{x}_{k-1}, \mathbf{u}_k) / g(\mathbf{x}_{k-1}, \mathbf{u}_k)$. We then assumed $\tilde{f}_{\mathbf{x}}^k$ and $\tilde{g}_{\mathbf{x}}^k$, two inputs to Algorithm 1, to be normal distributions and fitted the parameters of these distributions with conditional pdfs obtained from the data, i.e. $f(\mathbf{x}_k | \mathbf{x}_{k-1}, \mathbf{u}_k)$ and $g(\mathbf{x}_k | \mathbf{x}_{k-1}, \mathbf{u}_k)$ respectively. This yielded $\tilde{f}_{\mathbf{x}}^k \sim \mathcal{N}(a_c \mathbf{x}_{k-1} + b_c \mathbf{u}_k, \sigma_c^2)$, $\tilde{g}_{\mathbf{x}}^k \sim \mathcal{N}(a_e \mathbf{x}_{k-1} + b_e \mathbf{u}_k, \sigma_e^2)$ with $a_c = 0.9820$, $b_c = 0.2591$ s, $\sigma_c^2 = 2.6118$ m² and $a_e = 0.9811$, $b_e = 0.2723$ s, $\sigma_e^2 = 1.7622$ m². Finally, $\tilde{g}_{\mathbf{U}}^k$ was also com-

² See e.g. www.csselectronics.com/screen/page/simple-intro-obd2-explained/language/en

³ See <http://hybridassistant.blogspot.com/>

puted by conditioning, i.e. $\tilde{g}_{\mathbf{U}}^k = g(\mathbf{x}_{k-1}, \mathbf{u}_k) / g(\mathbf{x}_{k-1})$.

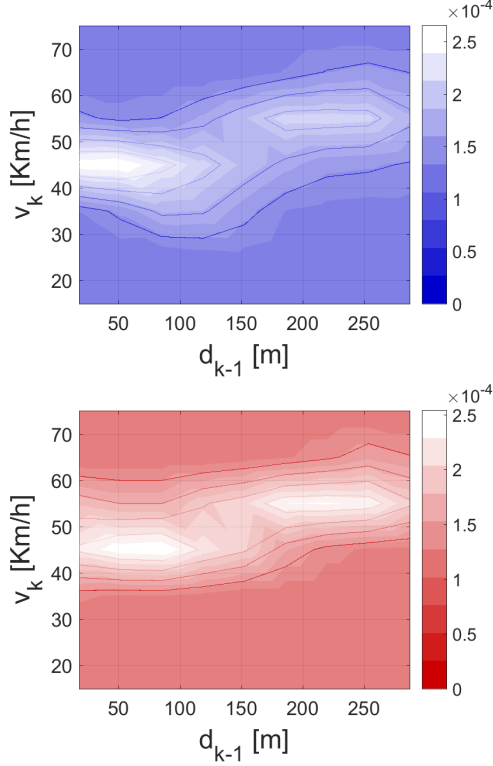


Fig. 4. Heat-maps for $f(\mathbf{x}_{k-1}, \mathbf{u}_k)$ (top panel) and $g(\mathbf{x}_{k-1}, \mathbf{u}_k)$ (bottom panel).

Synthesis of the control policy. Given this set-up, we used Algorithm 1 to solve Problem 1 and hence to synthesize from the examples a control policy allowing the car to merge on the highway. When synthesizing the control policy, we imposed a constraint on the variance of the control variable (see also Remark 5). In particular, we imposed the variance of $(\tilde{f}_{\mathbf{U}}^k)^*$, i.e. the pdf solving Problem 1 at time-step k , to be larger than the variance of $\tilde{g}_{\mathbf{U}}^k$. Physically, by imposing this constraint, we allowed the closed-loop system to have variations of the control variable larger than these observed in the examples, thus leading to a potentially more *aggressive* driving profile. We used Algorithm 1 to compute the sequence of pdfs solving Problem 1 and approximated these pdfs via the Maximum Entropy Principle. This resulted into the sequence of truncated Gaussians of Figure 5. In such a figure, it is clearly shown how these pdfs have higher variance than the corresponding $\tilde{g}_{\mathbf{U}}^k$ extracted from the examples. At each time-step, the control input, \mathbf{u}_k , applied to the car was obtained by sampling the pdfs of Figure 5. In particular, by taking the \mathbf{u}_k 's as the mean value of the random variable generated by these pdfs, we obtained the speed profile for the controlled car illustrated in Figure 6.

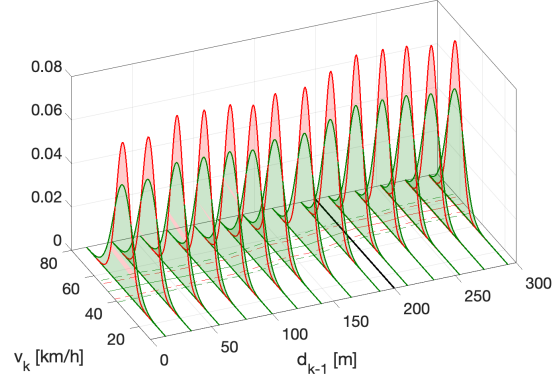


Fig. 5. The pdfs $\tilde{g}_{\mathbf{U}}^k$ from the examples (in red) together with the sequence of pdfs obtained from Algorithm 1 (green). For the sake of clarity in the figure, the pdfs are not shown for each iteration (the policies shown here are representative for all the other time-steps). The continuous line on the speed/distance plane denotes the expectation of the pdfs/policies, while the dashed lines represent the variance of the policies from the examples (red) and from Algorithm 1 (green). These are shown for each time-step.

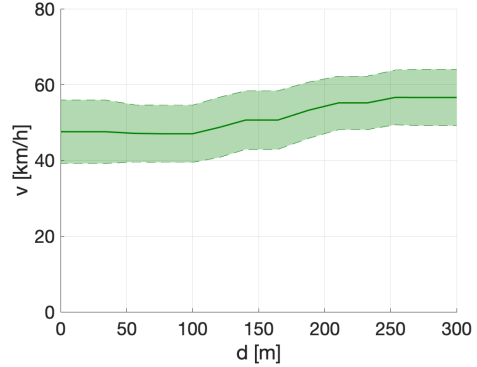


Fig. 6. Speed profile of the car across multiple simulations when \mathbf{u}_k is the expectation of the random value generated by $(\tilde{f}_{\mathbf{U}}^k)^*$. The bold line denotes the average of the profile and the shaded area represents the confidence interval corresponding to the standard deviation.

7 Conclusions

We considered the problem of synthesizing control policies from noisy example datasets for systems affected by actuation constraints. To tackle this problem, we introduced a number of technical results to explicitly compute the policy directly from certain pdfs obtained from the data and in compliance with the constraints. The results were also turned into an algorithmic procedure and their effectiveness was illustrated via a use-case. The use-case involved the synthesis, from measured data collected during test drives, of a control policy allowing a car to merge on a highway. Future work will be aimed at extending the results presented in this paper by consid-

ering: (i) the introduction of chance constraints on the state variable; (ii) resilience to data falsification attacks.

A Appendix: proofs of the technical results

Here we give the proofs for Property 1 and Lemma 1.

A.1 Proof of Property 1

To prove this result we start from the definition of KL-divergence. In particular:

$$\begin{aligned} \mathcal{D}_{\text{KL}}(\phi(\mathbf{y}, \mathbf{z}) || g(\mathbf{y}, \mathbf{z})) &:= \\ &= \int \int \phi(\mathbf{y}, \mathbf{z}) \left[\ln \frac{\phi(\mathbf{y}, \mathbf{z})}{g(\mathbf{y}, \mathbf{z})} \right] d\mathbf{y} d\mathbf{z} = \\ &= \int \int \phi(\mathbf{z}|\mathbf{y}) \phi(\mathbf{y}) \left[\ln \frac{\phi(\mathbf{z}|\mathbf{y})\phi(\mathbf{y})}{g(\mathbf{z}|\mathbf{y})g(\mathbf{y})} \right] d\mathbf{y} d\mathbf{z} = \\ &= \underbrace{\int \int \phi(\mathbf{z}|\mathbf{y}) \left[\phi(\mathbf{y}) \ln \frac{\phi(\mathbf{y})}{g(\mathbf{y})} \right] d\mathbf{y} d\mathbf{z}}_{(1)} + \\ &\quad + \underbrace{\int \int \phi(\mathbf{y}) \left[\phi(\mathbf{z}|\mathbf{y}) \ln \frac{\phi(\mathbf{z}|\mathbf{y})}{g(\mathbf{z}|\mathbf{y})} \right] d\mathbf{z} d\mathbf{y}}_{(2)}. \end{aligned}$$

For the term (1) in the above expression we may continue as follows:

$$\begin{aligned} \int \int \phi(\mathbf{z}|\mathbf{y}) \left[\phi(\mathbf{y}) \ln \frac{\phi(\mathbf{y})}{g(\mathbf{y})} \right] d\mathbf{y} d\mathbf{z} &= \\ &= \int \phi(\mathbf{z}|\mathbf{y}) d\mathbf{z} * \left[\int \phi(\mathbf{y}) \ln \frac{\phi(\mathbf{y})}{g(\mathbf{y})} d\mathbf{y} \right] = \\ &= \mathcal{D}_{\text{KL}}(\phi(\mathbf{y}) || g(\mathbf{y})) \end{aligned}$$

where we used Fubini's theorem, the fact that the term on the first line in square brackets is independent on \mathbf{Z} and the fact that $\int \phi(\mathbf{z}|\mathbf{y}) d\mathbf{z} = 1$. By using again Fubini's theorem, for the term (2) in the above expression instead we have:

$$\begin{aligned} \int \int \phi(\mathbf{y}) \left[\phi(\mathbf{z}|\mathbf{y}) \ln \frac{\phi(\mathbf{z}|\mathbf{y})}{g(\mathbf{z}|\mathbf{y})} \right] d\mathbf{z} d\mathbf{y} &= \\ &= \int \phi(\mathbf{y}) \left[\int \phi(\mathbf{z}|\mathbf{y}) \ln \frac{\phi(\mathbf{z}|\mathbf{y})}{g(\mathbf{z}|\mathbf{y})} d\mathbf{z} \right] d\mathbf{y} = \\ &= \int \phi(\mathbf{y}) [\mathcal{D}_{\text{KL}}(\phi(\mathbf{z}|\mathbf{y}) || g(\mathbf{z}|\mathbf{y}))] d\mathbf{y} = \\ &= \mathbb{E}_{\phi(\mathbf{Y})} [\mathcal{D}_{\text{KL}}(\phi(\mathbf{z}|\mathbf{Y}) || g(\mathbf{z}|\mathbf{Y}))], \end{aligned}$$

thus proving the result. \square

A.2 Proof of Lemma 1

The proof is organized in 3 steps. In **Step 1** we show that the optimization problem in (8) is a convex optimization problem (COP) and we then devise its augmented Lagrangian (this terminology is in accordance with (Kirk, 2004)). In **Step 2** we explicit the Karush-Kuhn-Tucker (KKT) conditions and verify that these

are satisfied by the solution in (11). Recall that for a COP KKT conditions are necessary and sufficient (Boyd and Vandenberghe, 2004, Chapter 5). Finally, in **Step 3**, we compute the minimum of the cost function corresponding to the optimal solution. We also recall that, in order to favour clarity in the expressions below, we omit the dependencies on the random vector \mathbf{Z} whenever this is clear from the context.

Step 1. We start with observing that the cost function $\mathcal{L}(f)$ in (8) can be conveniently rewritten as:

$$\mathcal{L}(f) = \int l(f) d\mathbf{z},$$

with

$$l(f) := f \left[\ln \left(\frac{f}{g} \right) + \alpha \right].$$

Clearly, $\mathcal{L}(\cdot)$ is twice differentiable and we now prove that it is also a strictly convex functional in f . We do this by showing that its second variation is positive definite on the space of integrable functions and we explicit the first and the second variation of \mathcal{L} (i.e. $\delta\mathcal{L}(f, \delta f)$ and $\delta^2\mathcal{L}(f, \delta f)$) in terms of the first and second derivative of $l(f)$ with respect to f (i.e. $\frac{\partial l(f)}{\partial f}$ and $\frac{\partial^2 l(f)}{\partial f^2}$, respectively). By computing $\delta\mathcal{L}$ we get:

$$\delta\mathcal{L}(f, \delta f) = \int \delta l(f, \delta f) d\mathbf{z} = \int \frac{\partial l(f)}{\partial f} [\delta f] d\mathbf{z},$$

with

$$\frac{\partial l(f)}{\partial f} = \ln f + (\alpha + 1 - \ln g).$$

This leads to the following expression for the second variation of \mathcal{L}

$$\delta^2\mathcal{L}(f, \delta f) = \int \delta^2 l(f, \delta f) d\mathbf{z} = \int \delta f \left(\frac{\partial^2 l}{\partial f^2} \right) \delta f d\mathbf{z} \quad (\text{A.1})$$

To show convexity of \mathcal{L} it then suffices to observe that, since f is positive on its support, then $\frac{\partial^2 l(f)}{\partial f^2} = \frac{1}{f}$ in (A.1) is non-negative. In turn, this implies that $\delta^2\mathcal{L}(f, \delta f)$ is strictly positive for any measurable, non-zero variation δf (see also (Kirk, 2004, Chapter 4) and (Giaquinta and Hildebrandt, 2004) for a detailed discussion). Hence, in order to conclude that the problem in (8) is a COP, it suffices to observe that the constraints in (10) are linear in f . The augmented Lagrangian of the COP in (8) is:

$$\mathcal{L}_{\text{aug}}(f, \boldsymbol{\lambda}) := \mathcal{L}(f) + \sum_{j \in \mathcal{E}_0 \cup \mathcal{I}} \lambda_j c_j[f], \quad (\text{A.2})$$

where $\boldsymbol{\lambda} := [\lambda_0, \lambda_1, \dots, \lambda_{n_e+n_l}]^T$ is the column vector stacking all the LMs.

Step 2. We showed that the problem in (8) is a COP and hence the KKT conditions are necessary and sufficient

<i>Primal feasibility:</i>	$c_j[f] = 0,$	$\forall j \in \mathcal{E}_0$
	$c_j[f] \leq 0,$	$\forall j \in \mathcal{I}$
<i>Dual feasibility:</i>	$\lambda_j \geq 0,$	$\forall j \in \mathcal{I}$
<i>Complementary slackness:</i>	$\lambda_j c_j[f] = 0,$	$\forall j \in \mathcal{I}$
<i>Stationarity:</i>	$\delta \mathcal{L}_{aug}(f, \delta f, \boldsymbol{\lambda}) = 0, \quad \forall \delta f$	

Table A.1

KKT conditions for the problem (8) - $\mathcal{L}_{aug}(f, \delta f, \boldsymbol{\lambda})$ is the augmented Lagrangian.

optimality conditions. That is, in order to be a unique minimizer of the problem (8), the candidate function f must satisfy the conditions made explicit in Table A.1.

We now impose the stationarity condition (see Table A.1) and first note that the augmented Lagrangian (A.2) can be written as follows:

$$\mathcal{L}_{aug}(f, \boldsymbol{\lambda}) := \int f \left[\ln \left(\frac{f}{g} \right) + \alpha \right] d\mathbf{z} + \langle \boldsymbol{\lambda}, \int f \mathbf{h}(\mathbf{z}) d\mathbf{z} - \mathbf{H} \rangle.$$

Hence, the above expression can be compactly rewritten as

$$\mathcal{L}_{aug}(f, \boldsymbol{\lambda}) = \int \tilde{l}(f, \boldsymbol{\lambda}) d\mathbf{z} - \langle \boldsymbol{\lambda}, \mathbf{H} \rangle, \quad (\text{A.3})$$

where the quantity under the integral is given by

$$\tilde{l}(f, \boldsymbol{\lambda}) := f \left[\ln \left(\frac{f}{g} \right) + \tilde{\alpha}(\boldsymbol{\lambda}) \right],$$

with

$$\tilde{\alpha}(\boldsymbol{\lambda}) = \alpha + \langle \boldsymbol{\lambda}, \mathbf{h} \rangle.$$

By computing the first variation of (A.3) with respect to δf we obtain

$$\delta \mathcal{L}_{aug}(f, \delta f, \boldsymbol{\lambda}) = \int \frac{\partial \tilde{l}(f, \boldsymbol{\lambda})}{\partial f} [\delta f] d\mathbf{z},$$

and thus, by imposing the stationarity (Nocedal and Wright, 2006) condition (i.e. $\delta \mathcal{L}_{aug}(f, \delta f, \boldsymbol{\lambda}) = 0, \forall \delta f$), we get $\frac{\partial \tilde{l}(f, \boldsymbol{\lambda})}{\partial f} = 0$. That is,

$$\frac{\partial \tilde{l}(f, \boldsymbol{\lambda})}{\partial f} = \ln \left(\frac{f}{g} \right) + \tilde{\alpha}(\boldsymbol{\lambda}) + 1 = 0,$$

from which it immediately follows that all the optimal solution candidates must be of the form $f = g e^{-\{1+\tilde{\alpha}(\boldsymbol{\lambda})\}}$, which, by definition of $\tilde{\alpha}$, becomes

$$f = g e^{-\{1+\alpha(\mathbf{z})+\langle \boldsymbol{\lambda}, \mathbf{h}(\mathbf{z}) \rangle\}} := \hat{f}^*(z, \boldsymbol{\lambda}). \quad (\text{A.4})$$

In the above expression, $\hat{f}^*(z, \boldsymbol{\lambda})$ was defined to stress that the optimal solution candidate is a function of the

LMs. These can be found by solving the following dual problem

$$\begin{aligned} \boldsymbol{\lambda}^* \in \arg \max_{\boldsymbol{\lambda}} \mathcal{L}^D(\boldsymbol{\lambda}) \\ \text{s.t.: } \lambda_j \text{ free}, \forall j \in \mathcal{E}_0, \\ \lambda_j \geq 0, \forall j \in \mathcal{I}, \end{aligned} \quad (\text{A.5})$$

choosing $\boldsymbol{\lambda}^*$ so that $\hat{f}^*(z, \boldsymbol{\lambda}^*)$ is primal feasible (see (Ben-Tal et al., 1988)). In the problem, $\mathcal{L}^D(\boldsymbol{\lambda})$ is the Lagrange dual function

$$\mathcal{L}^D(\boldsymbol{\lambda}) := \inf_{f \geq 0} \mathcal{L}_{aug}(f, \boldsymbol{\lambda}).$$

Note that the vector $\boldsymbol{\lambda}^*$ must satisfy the dual feasibility condition. Now, Assumption 1 implies strong duality (see Remark 3) and hence the complementary slackness condition (see Table A.1) is also fulfilled. Additionally, $\mathcal{L}_{aug}(f, \boldsymbol{\lambda})$ is strictly convex in f (indeed, its second variation with respect to δf is the same as the second variation of $\mathcal{L}(f)$), and hence $\inf_{f \geq 0} \mathcal{L}_{aug}(f, \boldsymbol{\lambda}) =$

$\mathcal{L}_{aug}(\hat{f}^*(z, \boldsymbol{\lambda}), \boldsymbol{\lambda})$. Thus:

$$\begin{aligned} \mathcal{L}^D(\boldsymbol{\lambda}) &= \mathcal{L}_{aug}(\hat{f}^*(z, \boldsymbol{\lambda}), \boldsymbol{\lambda}) \\ &= \int \hat{f}^*(\mathbf{z}, \boldsymbol{\lambda}) \left[\ln \left(\frac{g e^{-\{1+\tilde{\alpha}\}}}{g} \right) + \tilde{\alpha} \right] d\mathbf{z} - \langle \boldsymbol{\lambda}, \mathbf{H} \rangle \\ &= - \int \hat{f}^*(\mathbf{z}, \boldsymbol{\lambda}) d\mathbf{z} - \langle \boldsymbol{\lambda}, \mathbf{H} \rangle \\ &= - \int g \mathbf{z}(\mathbf{z}) e^{-\{1+\alpha(\mathbf{z})+\langle \boldsymbol{\lambda}, \mathbf{h}(\mathbf{z}) \rangle\}} d\mathbf{z} - \langle \boldsymbol{\lambda}, \mathbf{H} \rangle. \end{aligned} \quad (\text{A.6})$$

Note now that the last equivalence gives (14) in the statement of the lemma and hence the problem in (13). Moreover, the complementary slackness condition (CS) on the pair of optimizers $f^*, \boldsymbol{\lambda}^*$ implies, for a COP, that there is no duality gap. That is, $\mathcal{L}^D(\boldsymbol{\lambda}^*) = \mathcal{L}(f^*)$. In turn, this means that the LMs associated to inactive inequality constraints must be equal to 0, while all the LMs associated to active inequality constraints must be non-negative. Therefore, the optimal solution of the COP in (8) is given by

$$\hat{f}^*(\mathbf{z}, \boldsymbol{\lambda}^*) = f^* = g e^{-\left\{1+\alpha(\mathbf{z})+\sum_{j \in \mathcal{A}(f^*)} \lambda_j^* h_j(\mathbf{z})\right\}},$$

which was obtained by taking into account that only the LMs associated to the active constraints are non-zero. The above expression is equal to (11) where we highlighted the role of λ_0 as a normalization constant. This concludes the proof of **(R1)**.

Step 3. Finally, since there is no duality gap, the minimum value of the primal problem (i.e. the COP in (8))

can be obtained from (A.6). This leads to

$$\mathcal{L}^* := \mathcal{L}(f^*) = - \left(1 + \sum_{j \in \mathcal{A}(f^*)} \lambda_j^* H_j \right),$$

and thus completes the proof. \square

References

- Argall, B. D., Chernova, S., Veloso, M., Browning, B., 2009. A survey of robot learning from demonstration. *Robotics and Autonomous Systems* 57 (5), 469 – 483.
- Bae, I., Moon, J., Seo, J., 2019. Toward a comfortable driving experience for a self-driving shuttle bus. *Electronics* 8 (9), 943.
- Baggio, G., Katewa, V., Pasqualetti, F., 2019. Data-driven minimum-energy controls for linear systems. *IEEE Control Systems Letters* 3 (3), 589–594.
- Ben-Tal, A., Teboulle, M., Charnes, A., 1988. The role of duality in optimization problems involving entropy functionals with applications to information theory. *Journal of optimization theory and applications* 58, 209–223.
- Bot, R., Grad, S.-M., Wanka, G., 2005. Duality for optimization problems with entropy-like objective functions. *Journal of Information and Optimization Sciences* 22, 415–441.
- Boyd, S. P., Vandenberghe, L., 2004. *Convex optimization*. Cambridge university press.
- Bryson, A. E., June 1996. Optimal control-1950 to 1985. *IEEE Control Systems Magazine* 16 (3), 26–33.
- Censor, Y., Elfving, T., 1982. New methods for linear inequalities. *Linear Algebra and Its Applications* 42, 199–211.
- Coulson, J., Lygeros, J., Drfler, F., 2019. Data-enabled predictive control: In the shallows of the deepc. In: 2019 18th European Control Conference (ECC). pp. 307–312.
- Coulson, J., Lygeros, J., Drfler, F., 2019. Regularized and distributionally robust data-enabled predictive control.
- DelVecchio, D., Qian, Y., Murray, R. M., Sontag, E. D., 2018. Future systems and control research in synthetic biology. *Annual Reviews in Control* 45, 5 – 17.
- Duffin, R. J., Dantzig, G. B., Fan, K., 1956. Linear inequalities and related systems. No. 38. Princeton university press.
- Englert, P., Vien, N. A., Toussaint, M., 2017. Inverse kkt: Learning cost functions of manipulation tasks from demonstrations. *The International Journal of Robotics Research* 36 (13-14), 1474–1488.
- Fan, K., 1968. On infinite systems of linear inequalities. *Journal of Mathematical Analysis and Applications* 21 (3), 475–478.
- Fan, K., 1975. Two applications of a consistency theorem for systems of linear inequalities. *Linear Algebra and its Applications* 11 (2), 171–180.
- Gagliardi, D., Russo, G., 2020. On the synthesis of control policies from example datasets. In: 21st IFAC World Congress (to appear, see <https://arxiv.org/abs/2001.04428> for a preprint of an extended version with preliminary proofs).
- Giaquinta, M., Hildebrandt, S., 2004. *Calculus of variations II*. Vol. 311. Springer Science & Business Media.
- Gonçalves da Silva, G. R., Bazanella, A. S., Lorenzini, C., Campestri, L., 2019. Data-driven lqr control design. *IEEE Control Systems Letters* 3 (1), 180–185.
- Griggs, W., Ordóñez-Hurtado, R., Russo, G., Shorten, R., 2019. A vehicle-in-the-loop emulation platform for demonstrating intelligent transportation systems. In: *Control Strategies for Advanced Driver Assistance Systems and Autonomous Driving Functions*. Springer, pp. 133–154.
- Hanawal, M., Liu, H., Zhu, H., Paschalidis, I., 2019. Learning policies for Markov Decision Processes from data. *IEEE Transactions on Automatic Control* 64, 2298–2309.
- Hanawal, M. K., Liu, H., Zhu, H., Paschalidis, I. C., 2019. Learning policies for Markov Decision Processes from data. *IEEE Transactions on Automatic Control* 64 (6), 2298–2309.
- Herzallah, R., 2015. Fully probabilistic control for stochastic nonlinear control systems with input dependent noise. *Neural networks* 63, 199–207.
- Hiebert, K. L., 1980. Solving systems of linear equations and inequalities. *SIAM Journal on Numerical Analysis* 17 (3), 447–464.
- Hou, Z., Xu, J.-X., 2009. On data-driven control theory: the state of the art and perspective. *Acta Automatica Sinica* 35, 650–667.
- Hou, Z.-S., Wang, Z., 2013. From model-based control to data-driven control: Survey, classification and perspective. *Information Sciences* 235, 3 – 35, data-based Control, Decision, Scheduling and Fault Diagnostics.
- Kárný, M., 1996. Towards fully probabilistic control design. *Automatica* 32 (12), 1719–1722.
- Kárný, M., Guy, T. V., 2006. Fully probabilistic control design. *Systems & Control Letters* 55 (4), 259–265.
- Keel, L. H., Bhattacharyya, S. P., 2008. Controller synthesis free of analytical models: Three term controllers. *IEEE Transactions on Automatic Control* 53 (6), 1353–1369.
- Kirk, D. E., 2004. *Optimal control theory: an introduction*. Courier Corporation.
- Kullback, S., Leibler, R., 1951. On information and sufficiency. *Annals of Mathematical Statistics* 22, 79–87.
- Krn, M., Kroupa, T., 2012. Axiomatisation of fully probabilistic design. *Information Sciences* 186 (1), 105 – 113.
- LeBlanc, H. J., Zhang, H., Koutsoukos, X., Sundaram, S., 2013. Resilient asymptotic consensus in robust networks. *IEEE Journal on Selected Areas in Communications* 31 (4), 766–781.
- Markovsky, I., Rapisarda, P., 2007. On the linear quadratic data-driven control. In: 2007 European Control Conference (ECC). pp. 5313–5318.

- Nishiyama, T., 2020. Convex optimization on functionals of probability densities.
- Nocedal, J., Wright, S., 2006. Numerical optimization. Springer Science & Business Media.
- OpenStreetMap contributors, 2017. Planet dump retrieved from <https://planet.osm.org> . <https://www.openstreetmap.org>.
- Pegueroles, B. G., Russo, G., June 2019. On robust stability of fully probabilistic control with respect to data-driven model uncertainties. In: 2019 18th European Control Conference (ECC). pp. 2460–2465.
- Peterka, V., 1981. Bayesian approach to system identification. Elsevier, pp. 239–304.
- Ramachandran, D., Amir, E., 2007. Bayesian inverse reinforcement learning. In: Proceedings of the 20th International Joint Conference on Artificial Intelligence. IJCAI’07. Morgan Kaufmann Publishers Inc., San Francisco, CA, USA, pp. 2586–2591.
- Ratliff, N. D., Bagnell, J. A., Zinkevich, M. A., 2006. Maximum margin planning. In: Proceedings of the 23rd International Conference on Machine Learning. ICML ’06. ACM, New York, NY, USA, pp. 729–736.
- Ratliff, N. D., Silver, D., Bagnell, J. A., Jul 2009. Learning to search: Functional gradient techniques for imitation learning. *Autonomous Robots* 27 (1), 25–53.
- Rockafeller, R., 1976. Duality and stability in extremum problems involving convex functions. *Pacific Journal of Mathematics* 21, 167–186.
- Rosolia, U., Borrelli, F., 2018. Learning model predictive control for iterative tasks. a data-driven control framework. *IEEE Transactions on Automatic Control* 63 (7), 1883–1896.
- Salvador, J. R., delaPena, D. M., Alamo, T., Bemporad, A., 2018. Data-based predictive control via direct weight optimization. *IFAC-PapersOnLine* 51 (20), 356 – 361, 6th IFAC Conference on Nonlinear Model Predictive Control NMPC 2018.
- Singh, M., Vishnoi, N. K., 2014. Entropy, optimization and counting. In: Proceedings of the Forty-Sixth Annual ACM Symposium on Theory of Computing. STOC 14. Association for Computing Machinery, New York, NY, USA, p. 5059.
- Stdli, S., Seron, M., Middleton, R., 2017. From vehicular platoons to general networked systems: String stability and related concepts. *Annual Reviews in Control* 44, 157 – 172.
- Sutton, R. S., Barto, A. G., 1998. Introduction to Reinforcement Learning, 1st Edition. MIT Press, Cambridge, MA, USA.
- Tanaskovic, M., Fagiano, L., Novara, C., Morari, M., 2017. Data-driven control of nonlinear systems: An on-line direct approach. *Automatica* 75, 1 – 10.
- Van Waarde, H. J., Eising, J., Trentelman, H. L., Camlibel, M. K., 2020. Data informativity: a new perspective on data-driven analysis and control. *IEEE Transactions on Automatic Control*, 1–1.
- Wabersich, K. P., Zeilinger, M. N., June 2018. Scalable synthesis of safety certificates from data with application to learning-based control. In: 2018 European Control Conference (ECC). pp. 1691–1697.
- Xu, T., Paschalidis, I. C., June 2019. Learning models for writing better doctor prescriptions. In: 2019 18th European Control Conference (ECC). pp. 2454–2459.
- Zhu, H., Liu, H., Ataei, A., Munk, Y., Daniel, T., Paschalidis, I. C., 01 2020. Learning from animals: How to navigate complex terrains. *PLOS Computational Biology* 16 (1), 1–17.
- Ziebart, B. D., Maas, A., Bagnell, J. A., Dey, A. K., 2008. Maximum entropy inverse reinforcement learning. In: *Proc. AAAI*. pp. 1433–1438.
- Ziegler, J. G., Nichols, N. B., 1942. Optimum Settings for Automatic Controllers. *Transactions of the ASME* 64, 759768.